Journal of Clinical Gastroenterology and Hepatology

ISSN: 2575-7733

Open Access Research Article

CT-Based Radiomics Nomogram for Preoperative Evaluation of Overall Survival in Intrahepatic Cholangiocarcinoma after Surgical Resection

Yuguo Wei*

Department of Gastroenterology and Hepatology, University in Wuhan, Wuchang, China

ABSTRACT

Purpose: The purpose of this study was to establish a radiomics nomogram based on multi-phase contrast-enhanced Computed Tomography (CT) for preoperative prediction of Overall Survival (OS) in Intrahepatic Cholangiocarcinoma (ICC) after resection.

Methods: A cohort of 96 (7:3 in the training and validation cohorts) ICC patients was enrolled in this study. All patients underwent a preoperative enhanced CT examination and then accepted the ICC resection. Radiomics features were extracted from Arterial Phase (AP) and Portal Venous Phase (PVP) contrast-enhanced CT images, respectively. The Least Absolute Shrinkage and Selection Operator (LASSO) Cox regression was used to select the features. Radiomics and clinical features were combined to build the nomogram to predict the OS. ICC patients were divided into high and low risk groups based on cut-off value of the radscore. The Kaplan-Meier analysis and the log-rank test were applied to analyze the OS difference between different risk groups.

Results: Relative to the prediction of OS in ICC patients, the C-index of the radiomics was 0.869 in the training and 0.632 in the validation cohort, while the C-index of clinical-nomogram was 0.873 in the training and 0.628 in the validation cohorts. The C-index of the combined nomogram for the prediction of OS in ICC patients was 0.912 and 0.696 in the training and validation cohorts, respectively. The calibration curve indicated that the predicted survival time was close to the actual survival time. Decision curve analysis showed that the combined nomogram has better clinical prediction than clinical or radiomics features alone. The combined model showed that the low-risk group and high-risk group had a significant statistical difference in the OS of both training cohort ($p<0.001$) and validation cohort ($p=0.01$).

Conclusion: The newly developed clinical decision nomogram based on preoperative enhanced CT radiomics could not only be used to predict the OS of ICC, warn the risk factors affecting the survival status of ICC patients, but also play a certain role in assisting clinical treatment decision making.

Keywords: Intrahepatic cholangiocarcinoma; Computed tomography; Radiomics; Nomogram; Survival

Received:	15-June-2023	**Manuscript No:**	IPJCGH-23-16727
Editor assigned:	19-June-2023	**PreQC No:**	IPJCGH-23-16727 (PQ)
Reviewed:	03-July-2023	**QC No:**	IPJCGH-23-16727
Revised:	05-March-2024	**Manuscript No:**	IPJCGH-23-16727 (R)
Published:	12-March-2024	**DOI:**	10.36648/IPJCGH.8.2.12

Corresponding author: Yuguo Wei, Department of Gastroenterology and Hepatology, University in Wuhan, Wuchang, China; E-mail: ashishpanji@gmail.com

Citation: Wei Y (2024) CT-Based Radiomics Nosmogram for Preoperative Evaluation of Overall Survival in Intrahepatic Cholangiocarcinoma after Surgical Resection. J Clin Gastroenterol Hepatol. 8:12.

INTRODUCTION

Intrahepatic Cholangiocarcinoma (ICC) arises within the second order bile duct branches and peripheral branches and accounts for 5% to 30% of all primary liver malignancies [1-3]. It is a highly aggressive malignancy associated with high mortality and increasing global incidence in recent years [4]. Currently, surgical resection remains the best treatment choice. However, most ICC patients were usually diagnosed in advanced clinical stages, and only one third of patients could accept surgical resection. Unfortunately, the postoperative prognosis was disappointing, with the five-year survival and OS ranging from 15% to 40% [5]. Meanwhile, Adjuvant Therapy (AT) can only bring some survival benefits for unresectable patients, but whether postoperative AT is beneficial to patients after surgical resection is still controversial [6].

For ICC patients, accurate clinical staging is critical for predicting survival and selecting treatment options. Many recent studies have shown that the number of lesions, vascular invasion (e.g. microvascular or major vascular invasion), positive surgical margin, and lymph node metastasis are all important factors in ICC prognosis [7,8]. Therefore, imaging plays an important role in preoperation diagnosis and treatment of patients with suspected ICC. Multiphasic contrast enhanced multi-detector CT has high spatial resolution and advanced post-processing techniques and has served as the standard imaging modality for the preoperative assessment of ICC [9]. Meanwhile, the use of multi-detector CT can provide a comprehensive assessment and staging information of the primary tumor, the vascular and lymph node status, and the presence and extent of tumor invasion into the adjacent structures. In addition, based on the qualitative imaging features of ICC on CT, a better prediction of prognosis was identified in the survival outcomes of surgical patients [10]. However, the evaluation of these images is mostly dependent on the physicians, experience, which will affect the accuracy of the preoperative diagnosis. Therefore, there is an urgent need for an accurate and effective diagnostic method with higher clinical applicability and universality to preoperatively evaluate the OS.

In recent years, radiomics as an emerging and promising field, has shown discriminating capabilities in the stratification of tumor histology, tumor grades or stages, prognosis evaluation, and clinical treatment outcomes by extracting and mining large numbers of quantitative features from images [11,12]. In addition, the nomograms have been widely used as a reliable prediction tool to estimate prognosis in oncology and medicine by incorporating quantitative risk factors of clinical events [13]. Therefore, in this study, we extracted radiomics features from preoperative CT images of ICC in AP and PVP, respectively. Then, we established a radiomics nomogram combined with clinical factors to predict the survival status of ICC patients after resection.

MATERIALS AND METHODS

Patients

In this retrospective study, we reviewed clinical records, and AP and PVP contrast-enhanced CT images of ICC patients who underwent surgical resection between January 2011 and December 2018. The patients inclusion criteria were as follows: a) A multiphase enhanced CT examination within 1 month prior to surgery, b) No anti-tumor treatment received before the CT examination, c) Confirmed by pathology, d) With well-preserved imaging data, and clinical records. The exclusion criteria were as follows: a) With recurrent ICC; (b) Who underwent anti-tumor treatments before the contrast enhanced CT scan; and (c) With partial loss or poor CT images that could not be used for Region of Interest (ROI) delineation.

According to the above-mentioned inclusion-exclusion criteria, there were 96 ICC patients recruited. The patients were randomly split into training (n=68) and validation (n=28) cohorts in a 7:3 ratio. Clinical information, and radiologic findings were collected for each patient. Some potential factors for the prognosis of ICC were obtained, including age, sex, clinical symptoms, chronic hepatopathy history, Total Bilirubin (TBIL), Albumin (Alb), Globulin (GLB), Alanine Aminotransferase (ALT), Aspartate Aminotransferase (AST), Lymphocyte Count (LYM), neutrophils count, Platelet Count (PLT), Carcinoembryonic Antigen (CEA), Fetoprotein (AFP), Carbohydrate Antigen 19-9 (CA19-9), Carbohydrate Antigen 12-5 (CA12-5), growth patterns, number of the lesions, maximum diameter of the tumor, major vascular invasion, lymph node metastasis, adjacent organ invasion, distant metastasis, T stage, survival status. The preoperative serum CEA (abnormal or normal), AFP (abnormal or normal), CA19-9 (abnormal or normal), CA12-5 (abnormal or normal) were respectively achieved with the threshold value of 5 ng/ml, 20 u/ml, 37 u/ml, 35 u/ml in our institution. The endpoint of this study was OS, calculated as the time intervals between the date of surgery and the date of death or final follow-up. All patients were followed up until June 2021. The maximum follow-up time was 46 months (median, 25 months). The TNM stage of ICC was defined according to the TNM classification and staging system of the eighth edition by the American Joint Committee on Cancer (AJCC), which was mainly determined by surgical and pathological records.

CT Image Acquisition

All enrolled patients underwent contrast enhanced CT. All CT scans were performed on three CT scanners, including a 16-slice CT (Toshiba Medical Systems), a 64-slice CT (Revolution EVO, General Electric Medical Systems), and a 256-slice CT (Philips Healthcare). CT scans used the same scanning parameters: Tube voltage of 120 kV, tube current of 125-300 mAs, pitch of 0.6-1.25 mm, slice thickness of 3 mm, and reconstruction interval of 3 mm. Each patient was bolus injected (1.5 mL/kg) with the nonionic contrast agent ultravist 300 (Bayer Schering pharma) with a high pressure syringe at 3.0 mL/s. The AP and PVP were scanned at 25 to 35 seconds and 55 to 75 seconds after injection, respectively.

ROI Segmentation

Before radiomics features extraction, image resampling and gray level normalization were carried out to standardize different image specifications [14]. All image data were resampled to a 1 × 1 × 1 mm voxel space size. The gray scale was standardized to 64 levels to calculate the radiomics features.

The segmentation of tumor's ROI was contoured manually using ITK-SNAP software (version 3.8.0, http://www.itksnap.org/) [15]. The tumor boundary was outlined on each slice for both axial AP and PVP images by two abdominal radiologists (J.W., 9 years experience in abdominal radiology; W.X., more than 20 years experience in abdominal radiology). The two radiologists were aware of the final pathologic result, but they were blinded to the exact pathologic type and TNM stage.

Intra and Inter Observer Agreement

To evaluate the intra and inter observer agreement of radiomic features extraction, the intra and interclass correlation coefficients were calculated. 20 random images were chosen for ROI segmentation by two radiologists (reader A, 9 years experience in abdominal radiology; reader B, more than 20 years experience in abdominal radiology) to evaluate the interobserver agreement. A radiologist (A) repeated the same procedure in 20 random images two weeks later to assess the intra-observer agreement [16]. A value of the intra and interclass correlation coefficients greater than 0.8 was considered in good agreement.

Feature Extraction and Selection

Radiomics features including firstorder features, shape features, Gray-Level Co-occurrence Matrix (GLCM) features, Gray Level Size Zone Matrix (GLSZM) features, Gray Level Run Length Matrix (GLRLM) features, were extracted from the AP and PVP CT images separately based on segmented tumor ROIs using the Artificial Intelligence Kit Version 3.0.1.A (GE Healthcare, China), which based on pyradiomicss, and complies IBSI [17]. Ultimately, a total of 293 × 2 radiomics features were calculated and standardized. For the purpose of dimension reduction, a univariate cox regression analysis model was used to select the significant predictors from all the extracted image features. The correlation analysis between features was adopted, and one of the features with a correlation higher than 0.9 was retained to reduce the redundancy. Then, the survival analysis model was constructed by the Least Absolute Shrinkage and Selection Operator (LASSO) Cox regression analysis model. For each patient, a radiomics score (radscore) was produced using a linear combination of selected features that were weighted by their coefficients [18].

Construction of the Radiomicss Nomogram and its Performance

For clinical data, the univariate Cox regression analysis model was first used to select the significant predictors. Then, the multivariate Cox regression analysis model was adopted to develop the clinical survival analysis model.

The radscore from the radiomics model and predictors from the clinical survival model were used to construct the radiomics nomogram. In the training and validation cohorts, Harrell's C index was calculated to evaluate the predictive performance of the radiomics nomogram. The C-index is a number that varies from 0.5 to 1.0, with 0.5 denoting a random data distribution and 1.0 denoting that the model's results correctly match the observed survival data. Also, the radiomics nomogram calibration curves of the patient's 3-years OS were drawn [19]. The calibration curve showed the difference between the observed probabilities and the survival probability predicted by the nomogram. A decision curve was also applied to determine the clinical practicability of radiomicss nomogram by quantifying the net benefits under different threshold probabilities. The specific research process was shown in **Figure 1**.

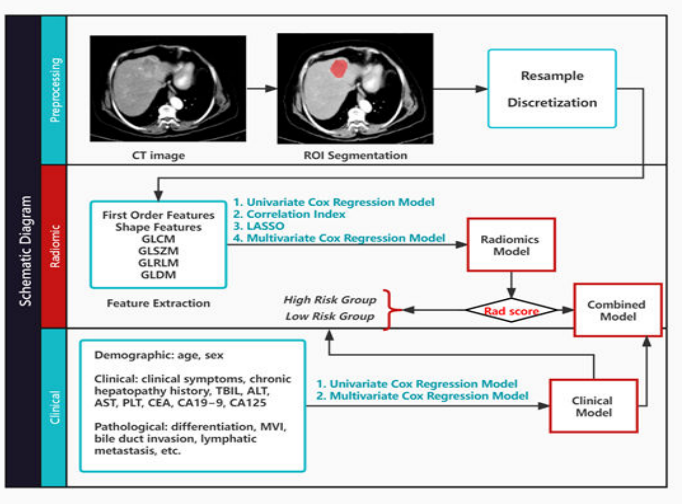

Figure 1: The workflow of model development.

Statistical Analysis

All statistical analyses were performed using the R software (version 4.0.2, www.r-progject.org) and Python (version 3.5.6). Mann-Whitney U test and χ^2 test were used to determine whether there was a significant difference in the values of clinical-pathologic variables. A two-tailed p-value <0.05 indicated statistical significance. The Kaplan-Meier analysis and a log-rank test were used to analyze the survival time and the difference between the patients from the high risk group and the low-risk group, in the training and the validation sets respectively.

RESULTS

Clinical Characteristics

The demographic and clinical characteristics of patients in the training and validation cohorts are summarized in **Table 1**, which indicated the distribution of all clinical characteristics were similar between the training and validation cohorts.

There were significant differences in age, clinical symptoms, Alb, CEA, CA 12-5, major vascular invasion, size, TNM stage, OS, and radscore between the survived and died cohorts ($p<0.05$).

Table 1: Clinical characteristics of the training and validation cohorts.

Variable	Training (n=68)	Validation (n=28)	Total (n=96)	p-value
Age (y), mean (sd) (%)	60.710 (10.290)	62.180 (8.190)	61.135 (9.685)	0.5
Sex (%)				
Male	37 (54.412)	15 (53.571)	52 (54.167)	
Female	31 (45.588)	13 (46.429)	44 (45.833)	1
Clinical symptoms (%)				
Asymptomatic	38 (55.882)	21 (75.000)	59 (61.458)	
Symptomatic	30 (44.118)	7 (25.000)	37 (38.542)	0.08
Chronic hepatopathy (%)	53 (77.941)	20 (71.429)	73 (76.042)	
Absent	53 (77.941)	20 (71.429)	73 (76.042)	
Hepatitis B associated liver cirrhosis	10 (14.706)	6 (21.429)	16 (16.667)	
Schistosomiasis cirrhosis of liver	4 (5.882)	2 (7.143)	6 (6.250)	
Primary biliary cirrhosis	1 (1.471)	0 (0.000)	1 (1.042)	0.775
TB (u mol/L), mean (sd)	27.025 (50.624)	31.039 (72.827)	28.196 (57.603)	0.757
Alb (g/L), mean (sd)	43.637 (4.838)	43.161 (6.499)	43.498 (5.344)	0.693
GLB, (g/L), mean (sd)	28.207 (4.093)	30.936 (9.901)	29.003 (6.421)	0.055
ALT, (IU/L), mean (sd)	37.706 (53.485)	38.429 (73.726)	37.917 (59.687)	0.957
AST, (IU/L), mean (sd)	40.088 (59.024)	31.714 (33.690)	37.646 (52.861)	0.482
LYM, (10^9/L), mean (sd)	1.573 (0.657)	1.661 (0.594)	1.599 (0.638)	0.543
Neutrophils (10^9/L), mean (sd)	4.273 (1.950)	4.068 (1.551)	4.213 (1.837)	0.62
PLT, (10^9/L), mean (sd)	203.676 (88.400)	194.857 (70.485)	201.104 (83.304)	0.639
CEA (u/ml)				
≤ 5	48 (70.588)	18 (64.286)	66 (68.750)	
>5	20 (29.412)	10 (35.714)	30 (31.250)	0.716
AFP (u/ml)				
≤ 20	63 (92.647)	27 (96.429)	90 (93.750)	
>20	5 (7.353)	1 (3.571)	6 (6.250)	0.817
CA199 (u/ml)				

≤ 37	31 (45.588)	14 (50.000)	45 (46.875)	
>37	37 (54.412)	14 (50.000)	51 (53.125)	0.866
CA125 (u/ml)				
≤ 35	46 (67.647)	22 (78.571)	68 (70.833)	
>35	22 (32.353)	6 (21.429)	28 (29.167)	0.41
Growth patterns				
Mass-forming	53 (77.941)	25 (89.286)	78 (81.250)	
Periductal infiltrating	12 (17.647)	3 (10.714)	15 (15.625)	
Intraductal growth	3 (4.412)	0 (0.000)	3 (3.125)	0.34
Number				
One	55 (80.882)	18 (64.286)	73 (76.042)	
Two	6 (8.824)	3 (10.714)	9 (9.375)	
More than two	7 (10.294)	7 (25.000)	14 (14.583)	0.155
Size (cm), mean (sd)	5.328 (2.016)	5.368 (2.801)	5.34 (2.257)	0.938
Adjacent organ invasion				
Absent	65 (95.588)	27 (96.429)	92 (95.833)	
Present	3 (4.412)	1 (3.571)	4 (4.167)	1
Major vascular invasion				
Absent	39 (57.353)	21 (75.000)	60 (62.500)	
Present	29 (42.647)	7 (25.000)	36 (37.500)	0.164
Lymphatic metastasis				
Absent	53 (77.941)	25 (89.286)	78 (81.250)	
Present	15 (22.059)	3 (10.714)	18 (18.750)	0.314
Distant metastasis				
Absent	67 (98.529)	27 (96.429)	94 (97.917)	
Present	1 (1.471)	1 (3.571)	2 (2.083)	1
TNM				
I	28 (41.176)	12 (42.857)	40 (41.667)	
II	17 (25.000)	10 (35.714)	27 (28.125)	
III	22 (32.353)	5 (17.857)	27 (28.125)	
IV	1 (1.471)	1 (3.571)	2 (2.083)	0.436
OS (month), mean (sd)	22.853 (13.371)	21.207 (11.126)	22.373 (12.722)	0.566
Radscore	0 (1.181)	0.126 (1.532)	0.037 (1.286)	0.663

Intra and Inter Observer Agreement

The intra observer consistency showed the intra class correlation coefficients was 0.850, and the inter observer correlation coefficients was 0.838. The results showed good intra- and inter observer agreement of the feature extraction.

Important Radiomics Feature Selection and Radiomics Signature Construction

Totally, 293 × 2 radiomics features were extracted from AP and PVP CT images separately. We used the LASSO regression model for feature selection (**Figures 2A and 2B**). Finally, nine important features were selected as follows (**Figure 2C**).

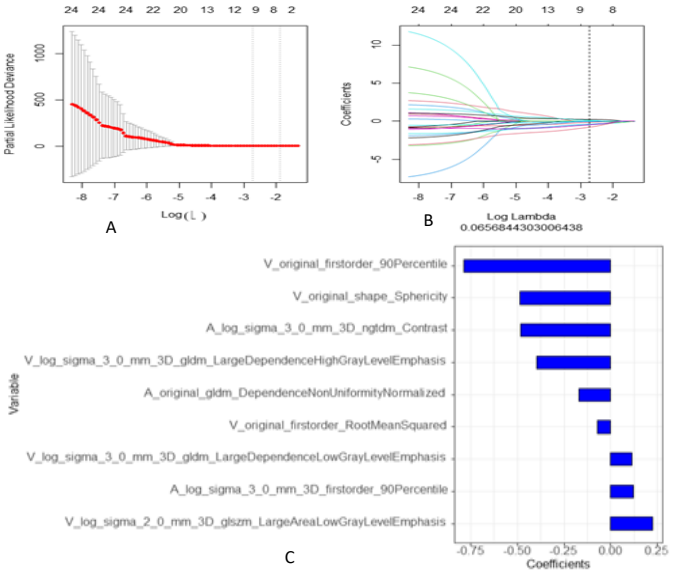

Figure 2: The optimal subset of radiomics features were extracted as shown. (A) The hyperparameter/lambda was determined using the partial likelihood deviation as the standard. (B) The optimization/lambda (vertical dotted line) was utilized to choose the features with non-zero coefficients. (C) The LASSO algorithm chose nine radiomics features that contributed the most to the prognosis prediction model.

Then the radscore were calculated as follows:

Radscore=0.227V_log_sigma_2_0_mm_3D_glszm_LargeAreaLowGrayLevelEmphasis +
0.124A_log_sigma_3_0_mm_3D_firstorder_90Percentile +
0.112V_log_sigma_3_0_mm_3D_gldm_LargeDependenceLowGrayLevelEmphasis −
0.071V_original_firstorder_RootMeanSquared −
0.172A_original_gldm_DependenceNonUniformityNormalized −
0.396V_log_sigma_3_0_mm_3D_gldm_LargeDependenceHighGrayLevelEmphasis −
0.484A_log_sigma_3_0_mm_3D_ngtdm_Contrast − 0.487V_original_shape_Sphericity −
0.788*V_original_firstorder_90Percentile.

The Kaplan-Meier analysis of the radiomics model was plotted to analyze the survival time between the patients from the high-risk group and the low-risk group in the training and validation sets, respectively. The results of the log rank test showed that there were significant differences between the two risk groups in the training set (p<0.01, log-rank test), but a trend to a significant result in the validation set (p=0.056, log-rank test).

Development of the Combined Nomogram and its Evaluation Performance

For all clinical data, we used the univariate Cox regression analysis model to select the significant predictor with P<0.05, and then utilized the multivariate Cox regression analysis model to construct the clinical nomogram (**Figure 3A**). The Kaplan-Meier curve showed that the combined model could effectively distinguish between high and low-risk patients in the test cohort (p<0.0001, log-rank test) (**Figure 3B**), but there was no statistical significance between low and high-risk group in the validation cohort (**Figure 3C**, p=0.31, log-rank test), which could be attributed to overfitting.

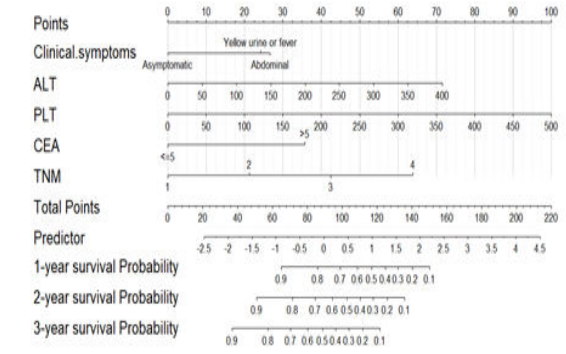

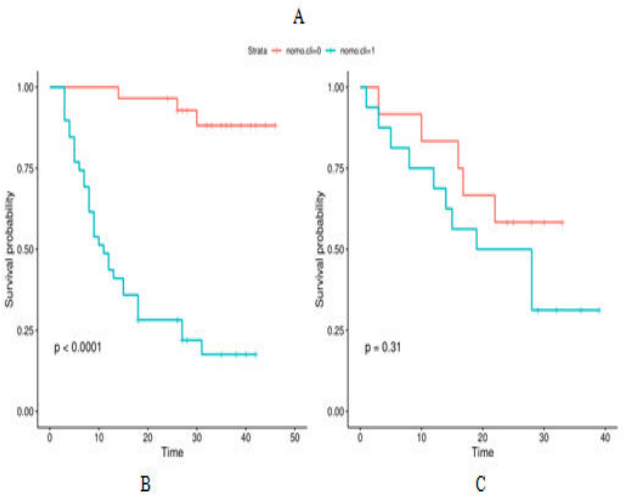

Figure 3: (A) A clinical logistic regression model for prediction of 1-3 years overall survival for ICC patients. (B) The Kaplan-Meier curve showed that the model could effectively distinguish between high and low-risk patients in test cohort (p<0.0001, log-rank test), (C) But there was no statistical significance in validation cohort (p=0.31, log-rank test).

Combining the radscore with the clinically significant predictors, a combined model was constructed based on multivariate Cox regression analysis (**Figure 4A**). In the training and validation cohorts, the C index of the combined model was 0.912 and 0.696, respectively (**Table 2**). The Kaplan-Meier curve demonstrated that the model score could effectively distinguish between high and low-risk patients in both the train cohort (**Figure 4B**, p<0.0001, log-rank test) and validation cohort (**Figure 4C**, p=0.01, log-rank test). The result of calibration curve indicated that the predicted probability was very close to the actual survival time of ICC patients (**Figure 4D**). The decision curve analysis showed that thecombined nomogram was better than the radiomics and clinical models and had a higher overall net benefit (**Figure 4E**).

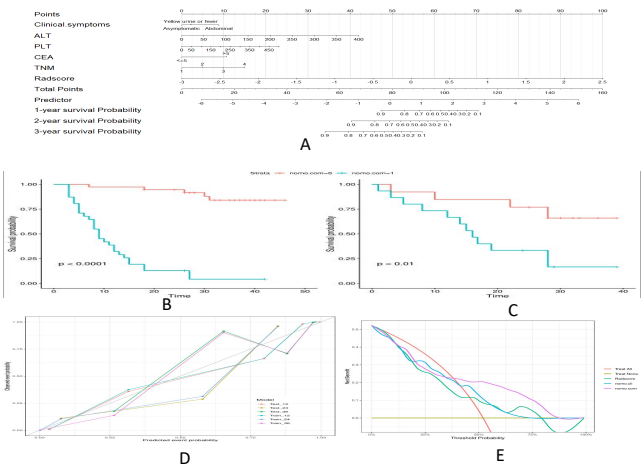

Figure 4: (A) A combined logistic regression model for prediction of 3 years overall survival for ICC patients. The Kaplan-Meier curve showed that the model could effectively distinguish between high and low-risk patients in test cohort (B) p<0.0001, log-rank test and validation cohort (C) p=0.01, log-rank test. (D) The result of calibration curve showed that the prediction probability was very close to the actual survival time of patients. (E) The decision curve analysis of each model showed that the combined nomogram was better than radiomics and clinical model, and had a higher overall net benefit.

Table 2: The comparison of prognostic accuracy between the combined model and two other prediction models.

	C-index	
	Training set	**Test set**
Radiomics	0.869 (se=0.026)	0.632 (se=0.072)
Clinical	0.873 (se=0.026)	0.628 (se=0.073)
Combined	0.912 (se=0.018)	0.696 (se=0.067)

DISCUSSION

ICC is the second most prevalent malignancy of primary liver cancer, only second to hepatocellular carcinoma [20]. Although its incidence is increasing in many geographic regions, its prognosis is generally poor, with a high rate of postoperative recurrence and high mortality [21]. In this study, we developed a combined model based on AP and PVP CT radiomics features combined with clinical factors to preoperative predict OS in patients with ICC after resection, with the aim of helping identify the patient who might benefit most from the surgical methods and guide personalized treatment.

In our study, the radiomics nomogram had a good predictive effect on the survival results of ICC patients, with the C-index 0.912 and 0.696 in the training and the validation set respectively. The results of this study indicated that compared with clinical features, radiomics signature was of great significance in evaluating the internal characteristics of tumors. It also indicated the potential of radiomics in predicting the survival outcome of preoperative ICC. We also found independent risk factors related to postoperative survival of ICC. Our combined model indicated that radscore and several clinical variables, including clinical symptoms, ALT, PLT, CEA, and TNM stages, were independent predictors of OS. The clinical characteristics of the survival and death cohorts highly suggested that radscore and some clinical factors, including clinical symptoms, CEA, and TNM stages, were closely related to the survival status of ICC patients after surgery.

Currently, surgery is still the first-line treatment for ICC, and it is also the best cure opportunity for ICC. However, most ICC patients usually had no symptoms in the early stages. When they developed symptoms such as abdominal pain, fatigue, malaise, and biliary obstruction, they were already in the advanced stage [19,22]. Our study also showed that the prognosis of ICC patients with first clinical symptoms was poor, which might be related to the poor physical condition and the late stage or metastasis of tumor.

Tumor markers are well-established tools for assisting in diagnosis, predicting prognosis, and detecting recurrence [23,24]. In our study, we found that serum biomarkers Alb,

CEA, and CA125 were related to the prognosis of patients. Among them, the level of Alb was considered to be the most important factor in assessing liver reserve, and decreased Alb indicated hepatocyte damage. According to a literature review, hypoproteinemia was an independent risk factor for increasing mortality and complications in critically ill patients [25]. Also, some studies found that hypoalbuminemia was associated with low survival in ICC patients [26], which was consistent with our research. As for tumor markers, it was considered that serum CA125 might have better clinical application in adenocarcinoma. A recent study has shown that preoperative serum CA125 could be used to predict the prognosis of hilar cholangiocarcinoma after radical resection [27]. A previous study showed that higher levels of CA19-9 and CEA were related to the advanced TNM stages and poor prognosis of ICC patients [28]. Nevertheless, there were some contradicting studies [29,30], a meta-analysis indicated that serum tumor markers did not help predict postoperative prognosis in patients with ICC [31]. But we also found the serum CA19-9 had no significant contribution in the clinical model and combined model.

Recently, several preoperative prediction models based on pretreatment enhanced CT have been developed for ICC patients, especially those who have undergone curative-intent resection, which suggested that artificial intelligence based on enhanced CT images had potential value in predicting the prognosis of some human diseases [32-34]. In addition, additional information extracted from radiomics can reveal the spatial heterogeneity within tumors and can be used to predict tumor type, tumor stage and prognosis [35]. Our study also found that the prognosis of patients with a high TNM stage was poor, and previous studies have confirmed that tumor size, multiple tumors, lymph node metastasis, vascular infiltration and poor tumor differentiation were related to the prognosis of ICC. Our findings have revealed more preoperative independent predictors of ICC, with clinical symptoms, ALT, and PLT not mentioned in other radiomics based studies. Our results also indicated that patients classified as high-risk group had higher risk of death events and worse prognosis than patients in low-risk group. These findings were consistent with previous radiomics studies [36]. Therefore, preoperative prediction of survival in ICC patients may facilitate clinical decision making. In this case, the prediction models and nomograms proposed in clinical practice or future clinical trials may help to identify the optimal candidates for surgery or high-risk patients.

Our study had several limitations. First, this study used a small sample and a retrospective design, so there may be potential selection bias. Moreover, the sample size was not large enough which alse caused the problem of overfitting in the test cohort. Second, this study was conducted in a single center. Both the overfitting problem and the single center study need the external validation using retained testing datasets or datasets from other hospital's to evaluate the predictive performance [37]. Third, there is no stratified analysis of some clinical indicators of ICC patients pre- and post- operation, such as preoperative CA 19-9 level, postoperative AT, prediction of postoperative tumor recurrence, which may lead to some discrepancies. In the follow-up study, we will increase the sample size, conduct multicenter and prospective researches, and design hierarchical analysis of relevant clinical, pathological, and radiomicss features in order to obtain more conclusive data on the prognosis of ICC patients.

CONCLUSION

In conclusion, a radscore based on enhanced CT combined with clinicopathological factors can predict the postoperative survival outcomes of ICC patients. The prediction result of the radiomicss nomogram might contribute to clinical decision making and identify the subgroups of patients who benefit most from surgery.

AUTHOR'S CONTRIBUTIONS

All authors contributed to the study conception and design. Material preparation, data collection and analysis were performed by WJ, MH, XZ, XW and ZX. The first draft of the manuscript was written by WJ and all authors commented on previous versions of the manuscript. All authors read and approved the final manuscript.

FUNDING

This study was funded by the horizontal project of Zhejiang university (Grant No. K-20212766).

DATA AVAILABILITY

The datasets analyzed in this study are available from the corresponding author on request.

CONFLICT OF INTEREST

The authors declare that they have no competing interests.

ETHICAL APPROVAL

All procedures performed in the study were in accordance with the Helsinki declaration and guidelines. The Clinical Research Ethics of the First Affiliated Hospital, Zhejiang University School of Medicine approved this retrospective study.

CONSENT TO PARTICIPATE

The requirement for patient informed consent was waived due to its retrospective nature.

CONSENT FOR PUBLICATION

All authors have read, reviewed, and approved of this manuscript for publication in its present form.

REFERENCES

1. Krasinskas AM (2018) Cholangiocarcinoma. Surg Pathol Clin. 11(2):403-429.
2. Liver cancer study group of Japan (1990) Primary liver cancer in Japan: Clinicopathologic features and results of surgical treatment. Ann Surg. 211(3):277-287.
3. Kaczynski J, Hansson G, Wallerstedt S (1998) Incidence, etiologic aspect and clinicopathologic features in intrahepatic cholangiocellular carcinoma-A study of 51 cases from a low-endemicity area. Acta Oncol. 37(1):77-83.
4. Spolverato G, Vitale A, Cucchetti A (2015) Can hepatic resection provide a long term cure for patients with intrahepatic cholangiocarcinoma? Cancer. 121(22):3998-4006.
5. Bridgewater J, Galle PR, Khan SA, Llovet JM, Park JW, et al. (2014) Guidelines for the diagnosis and management of intrahepatic cholangiocarcinoma. J Hepatol. 60(6):1268-1289.
6. Chun YS, Javle M (2017) Systemic and adjuvant therapies for intrahepatic cholangiocarcinoma. Cancer Control. 24(3).
7. Lee AJ, Chun YS (2018) Intrahepatic cholangiocarcinoma: The AJCC/UICC 8th edition updates. Chin Clin Oncol. 7(5):52.
8. Hwang S, Lee YJ, Song GW, Park KM, Kim KH, et al. (2015) Prognostic impact of tumor growth type on 7th AJCC staging system for intrahepatic cholangiocarcinoma: A single-center experience of 659 cases. J Gastrointest Surg. 19(7):1291-1304.
9. Joo I, Lee JM, Yoon JH (2018) Imaging diagnosis of intrahepatic and perihilar cholangiocarcinoma: Recent advances and challenges. Radiol. 288(1):7-13.
10. Aherne EA, Pak LM, Goldman DA, Gonen M, Jarnagin WR, et al. (2018) Intrahepatic cholangiocarcinoma: can imaging pheno-types predict survival and tumor genetics? Abdom Radiol (NY). 43(10):2665-2672.
11. Parmar C, Grossmann P, Bussink J, Lambin P, Aerts HJ (2015) Machine learning methods for quantitative radiomics biomarkers. Sci Rep. 5:13087.
12. Yang CM, Shu J (2021) Cholangiocarcinoma evaluation *via* imaging and artificial intelligence. Oncol. 99(2):72-83.
13. Balachandran VP, Gonen M, Smith JJ, deMatteo RP (2015) Nomograms in oncology: More than meets the eye. Lancet Oncol. 16(4):e173–e180.
14. Huynh E, Coroller TP, grawal V, Hou Y, Hou Y, et al. (2016) CT-based radiomics analysis of stereotactic body radiation therapy patients with lung cancer. Radiother Oncol. 120(2):258-266.
15. Yushkevich PA, Piven J, Hazlett, HC, Hazlett HC, Smith RG, et al. (2006) User-guided 3D active contour segmentation of anatomical structures: Significantly improved efficiency and reliability. NeuroImage. 31(3):1116-1128.
16. Guo Y, Chen X, Lin X, Chen L, Shu J, et al. (2021) Non-contrast CT-based radiomic signature for screening thoracic aortic dissections: A multicenter study. Eur Radiol. 31(9):7067-7076.
17. Griethuysen JJM, Fedorov A, Parmar C, Hosny A, Aucoin N, et al. (2017) Computational radiomicss system to decode the radiographic phenotype. Cancer Research 77(21): e104-e107.
18. Huang YQ, Liang CH, He L, Tian J, Liang CS, et al (2016) Development and validation of a radiomicss nomogram for preoperative prediction of lymph node metastasis in colorectal cancer. J Clin Oncol 34(18):2157-2164.
19. Yang L, Yang J, Zhou X, Huang L, Zhao W, et al. (2019) Development of a radiomicss nomogram based on the 2D and 3D CT features to predict the survival of non-small cell lung cancer patients. Eur Radiol 29(5):2196–2206.
20. Granata V, Grassi R, Fusco R (2021) Intrahepatic cholangiocarcinoma and its differential diagnosis at MRI: How radiologist should assess MR features. Radiol Med. 126:1584-1600.
21. Jin KP, Sheng RF, Yang C, Zeng MS (2022) Combined arterial and delayed enhancement patterns of MRI assist in prognostic prediction for Intrahepatic Mass-forming Cholangiocarcinoma (IMCC). Abdom Radiol (NY). 47(2):640-650.
22. Blechacz B (2017) Cholangiocarcinoma: Current knowledge and new developments. Gut Liver 11(1):13-26.
23. Fang T, Wang H, Wang Y, Lin X, Cui Y, et al. (2019) Clinical significance of preoperative serum CEA, CA125, and CA19-9 levels in predicting the resectability of cholangiocarcinoma. Dis Markers 2019:6016931.
24. Moro A, Mehta R, Sahara K, Tsilimigras DI, Paredes AZ, et al. (2020) The fimpact off preoperafive ca19-9 and cea on outcomes of patients with intrahepatic cholangiocarcinoma. Ann Surg Oncol. 27(8):2888-2901.
25. Wen J, Chen X, Wei S, Ma X, Zhao Y (2022) Research progress and treatment status of liver cirrhosis with hypoproteinemia. Evidence based complementary and alternative medicine. 2245491.
26. Li H, Wu JS, Wang XT, Lv P, Gong LS, et al. (2014) Factors predicting surgical resection in patients with intrahepatic cholangiocarcinoma and cirrhosis. J Invest Surg 27(4):219-225.
27. Xu ZL, Ou Y, Dai HS, Wan K, Bie P, et al. (2021) Elevated preoperative CA125 levels predicts poor prognosis of hilar cholangiocarcinoma receiving radical surgery. Clin Res Hepatol Gastroenterol 45(6):101695.
28. Tian M, Liu W, Tao C, Tang Z, Zhou Y, et al. (2020) Prediction of overall survival in resectable Intrahepatic cholangiocarcinoma: ISICC-applied prediction model. Cancer Sci. 111(4):1084-1092.
29. Loosen SH, Roderburg C, Kauertz KL, Koch A, Vucur M, et al. (2017) CEA but not CA19-9 is an independent prognostic factor in patients undergoing resection of cholangiocarcinoma. Sci Rep. 7(1):16975.
30. Bergquist JR, Ivanics T, Storlie CB, Groeschl RT, Tee MC, et al. (2016) Implications of CA19-9 elevation for survival, staging, and treatment sequencing in intrahepatic cholangiocarcinoma: A national cohort analysis. J Surg Oncol. 114(4):475-482.

31. Mavros MN, Economopoulos KP, Alexiou VG, Pawlik TM (2014) Treatment and prognosis for patients with intrahepatic cholangiocarcinoma: Systematic review and meta-analysis. JAMA Surg. 149(6):565-574.
32. Chu H, Liu Z, Liang W, Zhou Q, Zhang Y, et al. (2021) Radiomics using CT images for preoperative prediction of futile resection in intrahepatic cholangiocarcinoma. Eur Radiol. 31(4):2368-2376.
33. Park HJ, Park B, Park SY, Choi SH, Rhee H, et al. (2021) Preoperative prediction of postsurgical outcomes in mass-forming intrahepatic cholangiocarcinoma based on clinical, radiologic, and radiomics features. Eur Radiol. 31(11):8638-8648.
34. Tang Y, Zhang T, Zhou X, Zhao Y, Xu H, et al. (2021) The preoperative prognostic value of the radiomics nomogram based on CT combined with machine learning in patients with Intrahepatic cholangiocarcinoma. World J Surg Oncol. 19(1):45.
35. King MJ, Hectors S, Lee KM, Omidele O, Babb JS, et al. (2020) Outcomes assessment in intrahepatic cholangiocarcinoma using qualitative and quantitative imaging features. Cancer Imaging 20:43.
36. Zhang J, Wu Z, Zhang X, Liu S, Zhao J, et al. (2020) Machine learning: an approach to preoperatively predict PD-1/PD-L1 expression and outcome in intrahepatic cholangiocarcinoma using MRI biomarkers. ESMO Open. 5(6):e000910.
37. Luo Y, Chen S, Valdes G (2020) Machine learning for radiation outcome modeling and prediction. Med Phys. 47(5):e178-e184.